EPJ Web of Conferences **88**, 00025 (2015)
DOI: 10.1051/epjconf/20158800025

Alpha condensates and nonlocalized cluster structures

Yasuro Funaki

RIKEN, Nishina Center, Hirosawa 2-1, Wako 351-0198, Japan

Abstract

We discuss a container structure for non-gaslike cluster states, in which single Tohsaki-Horiuchi-Schuck-Röpke (THSR) wave functions are shown to be almost 100 % equivalent to the full solutions of the corresponding RGM/GCM equations, for the inversion doublet band states in ^{20}Ne, α-linear-chain states, and $\alpha+\alpha+\Lambda$ cluster states in $^{9}_{\Lambda}$Be. The recognition of the fact that the THSR wave function describes well not only gaslike cluster states but also non-gaslike cluster states is a recent remarkable development of nuclear cluster physics. This fact tells us that the cluster structure is composed of cluster-mean-field motion under the constraint of inter-cluster Pauli repulsion, in which we call the cluster-mean-field potential the container.

1 Introduction

The gaslike cluster structure is a novel type of nuclear clustering. The structure was first suggested in the study of ^{12}C, in which the Hoyle state (the second 0^+ state of ^{12}C at 7.65 MeV) was found to have a large root-mean-square (r.m.s.) radius and a loosely coupled S-wave component dominantly with respect to the relative α-α motions, like a gas. The microscopic cluster model calculations such as the resonating group method (RGM), generator coordinate method (GCM), and orthogonality condition model (OCM) reproduced almost of all experimental data available of the Hoyle state and revealed its structure [1]. After that, about 20 years later, the Hoyle state was reinvestigated by using the α-condensation-like wave function, which

we now refer to as the Tohsaki-Horiuchi-Schuck-Röpke (THSR) wave function [2], focusing on an analogy to the α condensation in nuclear matter [3]. After it was found in 2003 that the fully-microscopic wave functions of the 3α RGM and GCM obtained long time ago are almost 100 % equivalent to single THSR wave functions, we have had a new understanding of the Hoyle state that is the 3α condensate, where the 3α particles loosely couple with each other like a gas and occupy the lowest energy S-orbit of mean-field-like single-α potential [4]. This equivalence relation of the RGM/GCM wave function to single THSR wave function is also found in the case of ^{8}Be ground state [5].

In contrast, non-gaslike cluster states have been recognized as having localized structures of clusters, which are obviously quite different from the α condensate states mentioned above. A typical example is the inversion doublet band states of $\alpha + {}^{16}$O in ^{20}Ne [6], which have parity-violating intrinsic deformation. Another example is a linear-chain-state of α particles, where all α clusters are aligned on a line with a rigid-body configuration [7]. ${}^{9}_{\Lambda}$Be nucleus is also such an example, where the additional Λ particle shrinks the core ^{8}Be and compact and non-gaslike 2α cluster structure seems to be realized. Thus, the concept of the localized clustering is the important basis to understand these structure states. The very recent calculations, however, upset this common sense by revealing that all those structure states can also be represented by the single configurations of the THSR wave function with nearly 100 % accuracy [8–12]. The THSR wave function has a container structure that the clusters are nonlocalized and move around in a whole nuclear volume (container) characterized by a size parameter "B". We will report in this contribution that the container structure is realized not only for the gaslike cluster states but also for the non-gaslike cluster states, by showing that the THSR-type wave functions describe well non-gaslike cluster states mentioned above.

2 THSR description of inversion-doublet bands in ^{20}Ne

In this section, we show that the ^{16}O + α Brink-GCM wave functions of the states belonging to the inversion-doublet bands of ^{20}Ne have almost 100% square overlaps with single THSR wave functions. The THSR wave function was introduced in order to describe cluster-gaslike states, especially α-condensate-like states.

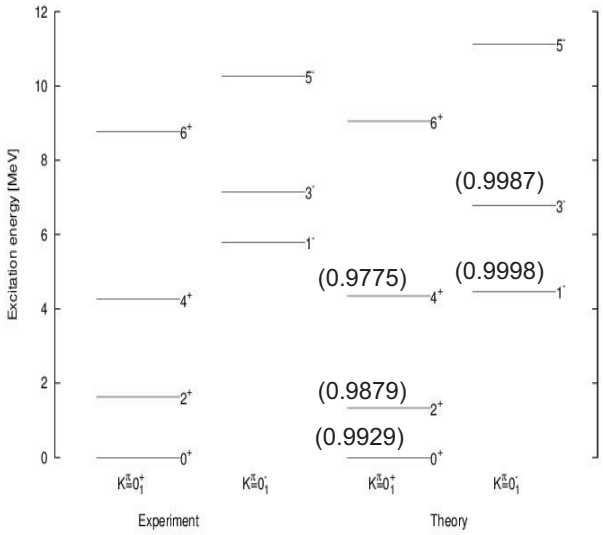

Figure 1: Comparison of the energy spectrum of inversion-doublet rotational bands in ^{20}Ne between experiment and theory. The squared overlap values between the single THSR wave functions and Brink-GCM wave functions are shown in parentheses.

The THSR wave function of ^{16}O + α clustering is given by

$$\Psi^{\mathrm{THSR},(J^-)} = C_J P^J_{M0} \int d\boldsymbol{R}\ \exp\left\{-\frac{4(R_x^2+R_y^2)}{5\beta_x^2}-\frac{4R_z^2}{5\beta_z^2}\right\}\Psi^{\mathrm{B}}_{^{16}\mathrm{O}+\alpha}\Big(\frac{4}{5}\boldsymbol{R},-\frac{1}{5}\boldsymbol{R}\Big), \quad (1)$$
$$= C'_J \exp(-\frac{10}{b^2}\boldsymbol{X}_G^2)\ P^J_{M0}\ \mathcal{A}\left[\exp\left\{-\frac{8(r_x^2+r_y^2)}{5B_x^2}-\frac{8r_z^2}{5B_z^2}\right\}\ \phi(^{16}\mathrm{O})\phi(\alpha)\right],$$

where $B_k^2 = b^2 + 2\beta_k^2$ $(k = x, y, z)$, $\boldsymbol{r} = \boldsymbol{X}_\alpha - \boldsymbol{X}_\mathrm{O}$, and $\boldsymbol{X}_G$ is total c.o.m. coordinate. $\Psi^{\mathrm{B}}_{^{16}\mathrm{O}+\alpha}(\frac{4}{5}\boldsymbol{R},-\frac{1}{5}\boldsymbol{R})$ is the $\alpha + {}^{16}$O Brink wave function and C_J and C'_J are normalization constants. This THSR wave function Ψ^{THSR}_J has positive parity and therefore can have only even angular momentum J. The negative-parity THSR wave function with odd J is constructed by the following procedure

$$\Phi^{\mathrm{THSR},(J^-)} = \lim_{S_z\to 0} C_J^{(-)}\ P^J_{M0}\ \frac{1-P_\pi}{2} \times$$
$$\mathcal{A}\left[\exp\left\{-\frac{8(r_x^2+r_y^2)}{5B_x^2} - \frac{8(r_z-S_z)^2}{5B_z^2}\right\}\ \phi(^{16}\mathrm{O})\phi(\alpha)\right], \qquad (2)$$

where $C_J^{(-)}$ is normalization constant and $(1-P_\pi)/2$ is the projection operator onto negative parity. If $B_x = B_z = B$, $\Phi^{\mathrm{THSR},(J^-)}$ has the following form

$$\Phi^{\mathrm{THSR},(J^-)} = D_J^{(-)}\mathcal{A}\left[r^J Y_{JM}(\hat{r})\ \exp\left\{-\frac{8r^2}{5B^2}\right\}\ \phi(^{16}\mathrm{O})\phi(\alpha)\right]. \qquad (3)$$

In Fig. 1, we show the calculated energy spectrum in comparison with the experimental data. The squared overlap values of the single THSR wave function with the $\alpha+^{16}$O Brink-GCM wave function are shown in parentheses. As mentioned above, we can see that both wave functions are almost 100 % equivalent to each other. The inversion-doublet rotational bands in ^{20}Ne consist of the plus-parity band which is the ground-state band and the minus-parity band which is the $K^\pi = 0^-$ band upon the 1^- state at $E_x = 5.80$ MeV. The minus-parity band levels are all above the $^{16}\mathrm{O} + \alpha$ threshold and have large α-decay widths whose reduced widths are comparable with the Wigner limit value. In general the inversion-doublet rotational bands are generated from a parity-violating intrinsic deformed state. As the parity-violating intrinsic state of the inversion-doublet bands, spatially-localized cluster structure of $^{16}\mathrm{O} + \alpha$ is assigned [6]. Therefore the existence of the inversion-doublet rotational bands has been regarded as a convincing evidence of the spatial localization of clusters. On the other hand, the THSR wave function describes the nonlocalized motion of clusters. The almost 100% equivalence of the Brink-GCM wave functions and single THSR wave functions for the ^{20}Ne inversion-doublet band states is thus really striking.

The problem of localized clustering vs nonlocalized clustering was already noticed in 2002 in the THSR study of α-α clustering in ^{8}Be. Ref. [5] reported that the Brink-GCM wave function of the ground state of ^{8}Be is 100% equivalent to single THSR wave function. This equivalence looks like questioning the well-known dumbbell picture for the intrinsic shape of ^{8}Be. However it was shown recently [10] that the nucleon-density distribution of the intrinsic THSR wave function of 2α ground state displays clearly localized clustering of α-α as seen in Fig. 2 (left). The reason why the THSR

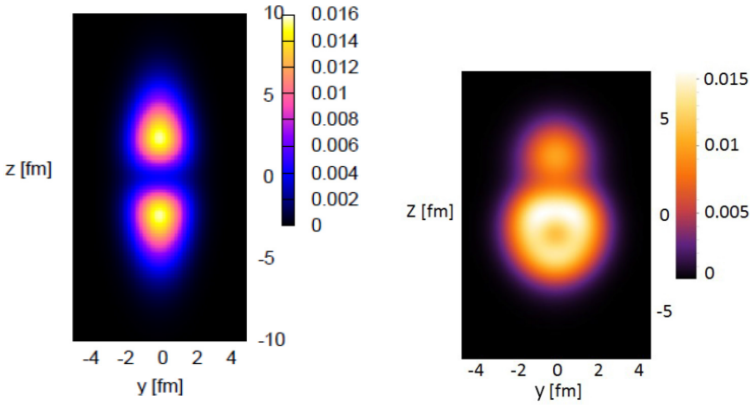

Figure 2: Nucleon-density distribution of the 2α prolate THSR wave function with $(\beta_x, \beta_y, \beta_z) = (1.78, 1.78, 8.75$ fm) [10] (left). Nucleon-density distribution of the ^{16}O + α hybrid-Brink-THSR wave function with $S_z = 0.6$ fm and $(\beta_x, \beta_y, \beta_z) = (0.9, 0.9, 2.5$ fm) [10] (right).

wave function which adopts the relative-motion wave function expressing the nonlocalized clustering yields the nucleon-density distribution showing the localized clustering is attributed to the inter-cluster Pauli repulsion which makes two clusters stay apart from each other avoiding close coming to each other. In the case of ^{20}Ne, for drawing the nucleon-density distribution of the intrinsic THSR wave function, we need a slight device because the THSR wave function is parity-symmetric as seen in Eq. (2) and cannot show parity-violating localized clustering of ^{16}O + α. The device we use is the following intrinsic hybrid-Brink-THSR wave function of ^{16}O + α:

$$\Phi^{\mathrm{hyb-B-THSR}} = \mathcal{A}\left[\exp\left\{-\frac{8(r_x^2+r_y^2)}{5B_x^2} - \frac{8(r_z-S_z)^2}{5B_z^2}\right\}\phi(^{16}\mathrm{O})\phi(\alpha)\right]. \quad (4)$$

Figure 2 (right) shows the nucleon-density distribution of the ^{16}O + α hybrid-Brink-THSR wave function with $S_z = 0.6$ fm and $(\beta_x, \beta_y, \beta_z) = (0.9, 0.9, 2.5$ fm) [10]. We observe in this figure that, in spite of the small value of $S_z = 0.6$ fm, the inter-cluster distance between ^{16}O and α is about 3.6 fm. Clearly the large inter-cluster distance of about 3.6 fm cannot be attributed to the small value of $S_z = 0.6$ fm, but should be attributed to the effective spatial localization of ^{16}O and α clusters in the prolate THSR wave function with $(\beta_x, \beta_y, \beta_z) = (0.9, 0.9, 2.5$ fm) with $S_z = 0$ which is just the intrinsic THSR wave function giving the minimum energy for the 0^+ state.

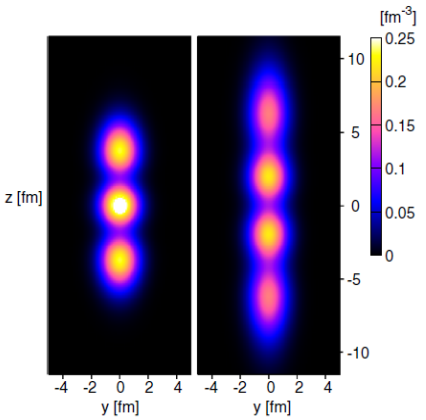

Figure 3: Intrinsic density profiles of the 3α- (Left) and 4α- (Right) linear-chain states from the THSR wave functions before angular-momentum projection at ($\beta_x = \beta_y$=0.1 fm,β_z=5.1 fm) and at ($\beta_x = \beta_y$=0.1 fm,β_z=8.2 fm), respectively. Figure taken from Ref. [11].

3 THSR description of 3α and 4α linear-chain states

If we follow the conclusion of the study of the inversion doublet bands of ^{20}Ne, the basic feature of the cluster dynamics is nonlocalized clustering and the localization of clusters is due to the inter-cluster Pauli repulsion. A confirmation of this conclusion was given in Ref. [11] by the investigation of the linear-chain structure of α clusters which is a typical and well-known example of localized cluster structure. It was reported that the Brink-GCM wave functions of the 3α and 4α linear-chain states have about 98 % and 94 % square overlaps with 3α and 4α single THSR wave functions, respectively. These large overlap values are to be compared with the maximum square overlap values with 3α and 4α single Brink wave functions which are 78 % and 48 %, respectively. These results urge us to regard that the Brink-GCM wave functions of the 3α and 4α linear-chain states have one-dimensional α-condensate-like character rather than the conventional picture of localized α clusters on a line. However, just like the case of ^{16}O + α inversion doublet, the nucleon-density distribution of the intrinsic THSR wave functions of linear-chain states show the localized α clusters because of inter-α Pauli repulsion, which is displayed in Fig. 3.

4 Conclusion

We demonstrated that the single THSR wave functions is almost 100 % equivalent to the full solutions of the RGM/GCM equations for the inversion doublet band states in ^{20}Ne and α-linear-chain states. The recognition of the fact that the THSR wave function describes well not only cluster-gaslike states but also non-gaslike cluster states is a recent remarkable development of nuclear cluster physics. This fact tells us that the cluster structure is composed of cluster-mean-field motion under the constraint of inter-cluster Pauli repulsion. The single-cluster wave function is the Gaussian wave packet around the c.o.m. coordinate which is the lowest orbit of the cluster-mean-field potential that we call the container.

References

[1] Fujiwara Y., Horiuchi H., Ikeda K., Kamimura M., Katō K., Suzuki Y., and Uegaki E., *Prog. Theor. Phys. Supple.* 68 (1980) Chapt.2, p.29

[2] Tohsaki A., Horiuchi H., Schuck P., and Röpke G., *Phys. Rev. Lett.* **87** (2001) 192501

[3] Röpke G., Schenell A., Schuck P., and Nozières P., *Phys. Rev. Lett.* **80** (1998) 3177

[4] Funaki Y., Tohsaki A., Horiuchi H., Schuck P., and Röpke G., *Phys. Rev.* C **67** (2003) 051306(R)

[5] Funaki Y., Horiuchi H., Tohsaki A., Schuck P., and Röpke G., *Prog. Theor. Phys.* **108** (2002) 297

[6] Horiuchi H. and Ikeda K., *Prog. Theor. Phys.* **40** (1968) 277

[7] Morinaga H., *Phys. Lett.* **21** (1966) 78

[8] Zhou B., Funaki Y., Horiuchi H., Ren Z., Röpke G., Schuck P., Tohsaki A., Xu C., and Yamada T., *Phys. Rev.* C **86** (2012) 014301

[9] Zhou B., Funaki Y., Horiuchi H., Ren Z., Röpke G., Schuck P., Tohsaki A., Xu C., and Yamada T., *Phys. Rev. Lett.* **110** (2013) 262501

[10] Zhou B., Funaki Y., Horiuchi H., Ren Z., Röpke G., Schuck P., Tohsaki A., Xu C., and Yamada T., *Phys. Rev.* C **89** (2014) 034319

[11] Suhara T., Funaki Y., Zhou B., Horiuchi H., and Tohsaki A., *Phys. Rev. Lett.* **112** (2014) 062501

[12] Funaki Y., Yamada T., Hiyama E., Zhou B., and Ikeda K., arXiv: 1405.6067, to appear in 2014 *Prog. Theor. Ext. Phys.*